2010

Bennett clocking of nanomagnetic logic using multiferroic single-domain nanomagnets

Jayasimha Atulasimha
Virginia Commonwealth University, jatulasimha@vcu.edu

Supriyo Bandyopadhyay
Virginia Commonwealth University, sbandy@vcu.edu

Atulasimha, J. and Bandyopadhyay, S. Bennett clocking of nanomagnetic logic using multiferroic single-domain nanomagnets. Applied Physics Letters, 97, 173105 (2010).

Bennett clocking of nanomagnetic logic using multiferroic single-domain nanomagnets

J. Atulasimha[1,a] and S. Bandyopadhyay[2]
[1]*Department of Mechanical Engineering, Virginia Commonwealth University, Richmond, Virginia 23284, USA*
[2]*Department of Electrical and Computer Engineering, Virginia Commonwealth University, Richmond, Virginia 23284, USA*

(Received 28 May 2010; accepted 5 October 2010; published online 26 October 2010)

The authors show that it is possible to rotate the magnetization of a multiferroic (strain-coupled two-layer magnetostrictive-piezoelectric) nanomagnet by a large angle with a small electrostatic potential. This can implement Bennett clocking [Int. J. Theor. Phys. **21**, 905 (1982)] in nanomagnetic logic arrays resulting in unidirectional propagation of logic bits from one stage to another. This method is potentially more energy efficient than using spin-transfer torque for magnetization rotation. For realistic parameters, it is shown that a potential of ~0.2 V applied to a multiferroic nanomagnet can rotate magnetization by nearly 90° to implement Bennett clocking. © *2010 American Institute of Physics*. [doi:10.1063/1.3506690]

Nanomagnetic logic—also known as magnetic quantum cellular automata[1]—is an energy-efficient computing paradigm that can work at room temperature.[1–6] In this architecture, classical binary bits 0 and 1 are encoded in two stable magnetization orientations parallel and antiparallel to the easy axis of magnetization of a nanomagnet with large shape anisotropy. Logic gates are configured by exploiting the dipole–dipole interaction between nearest neighbor nanomagnets.[1,2]

In order to propagate logic bits unidirectionally down a chain of nanomagnets, one requires a clock that periodically reorients every magnet's magnetization along the hard axis either with a global magnetic field that acts on all magnets simultaneously,[2] or with a local agent that acts on each magnetic independently.[3] The former does not allow pipelining data and requires materials with biaxial anisotropy,[7] to create a local minimum around the hard axis so that a magnet stays magnetized along this axis until a bit has propagated through it. Unfortunately, this minimum is so shallow that thermal noise can relax the magnetization quickly causing large bit error probability.[8] Therefore, we will consider only local clocking schemes, the most effective of which is due to Bennett.[9] To understand how Bennett clocking works, consider a nanomagnet array in the ground state shown in the first row of Fig. 1. In this state, the magnetizations of nearest neighbors are antiparallel owing to dipole–dipole interaction (Fig. 1; first row). As a result, the logic bit encoded in the magnetization orientation of the first nanomagnet is replicated in every odd-numbered nanomagnet. Therefore, this array acts like a wire (or a series of delay-gates) to transmit the first bit down the chain.

If we flip the magnetization of the first nanomagnet to switch its bit state (Fig. 1; second row), we expect all succeeding nanomagnets to flip in a domino effect so that the new bit state is propagated down the chain. However, this may not happen; the second magnet's magnetization does not necessarily flip since the second magnet finds its left neighbor telling it to flip, while its right neighbor (still in its original state) forbids flipping. Since both influences are equally strong (and the second magnet experiences no *net* dipole interaction), the array is stuck in a metastable state and the logic wire fails. To break this logjam, one forcibly turns the magnetizations of the second and third nanomagnet by a large angle with a local agent acting as a "clock" (Fig. 1; third row). When this agent is finally removed from the second nanomagnet, the latter finds itself in an asymmetric environment (left neighbor magnetized along easy axis and right neighbor close to the hard axis) which allows it to flip its magnetization (Fig. 1; fourth row) and reach the lowest energy state which will be the desired logic state. Thus, by sequentially rotating the magnetizations of magnet-pairs through a large angle (with a multiphase clock), one can propagate the new state of the first nanomagnet (input logic bit) unidirectionally down the chain. This is the essence of Bennett clocking.

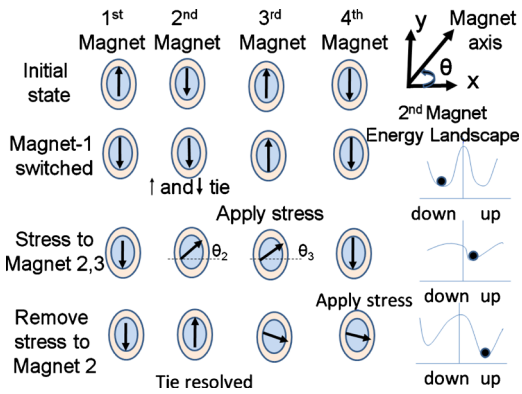

FIG. 1. (Color online) Logic propagation with Bennett clocking. (First row) A chain of elliptical nanomagnets in the ground state with magnetization orientation indicated by arrows. (Second row) Magnetization of the first magnet is flipped with an external agent and the second magnet finds itself in a tied state where it experiences no net dipole interaction. (Third row) The second and the third magnet are subjected to electrically induced stresses that rotate their magnetizations. (Fourth row) The second magnet is freed from stress and it switches to the desired "up" state since the dipole interaction from the left neighbor is now stronger than that from the right neighbor so that the tie is resolved. The right panel shows the energy landscape of the second magnet corresponding to the rows.

[a]Author to whom correspondence should be addressed. Electronic mail: jatulasimha@vcu.edu.

In this letter, we show that if a nanomagnet is composed of a multiferroic material,[10,11] then its magnetization can be rotated through large angles[12] by the stress generated in the magnetostrictive layer when the piezoelectric layer is subjected to an electrostatic potential. We also show that this can propagate logic bits unidirectionally and implement Bennett clocking.

Consider a chain of single-domain multiferroic nanomagnets as shown in Fig. 1. The total energy of any nanomagnet in this chain, subjected to a stress generated by an electrostatic potential, is $E_{\text{total}}=E_{\text{dipole}}+E_{\text{shape-anisotropy}}+E_{\text{stress-anisotropy}}$, where E_{dipole} is the dipole–dipole interaction energy between nearest neighbors, $E_{\text{shape-anisotropy}}$ is the shape anisotropy energy due to the magnet's anisotropic shape, and $E_{\text{stress-anisotropy}}$ is the stress anisotropy energy caused by the electrostatic potential generating stress. We neglect magnetocrystalline anisotropy terms assuming that the material is polycrystalline and we also neglect thermal fluctuations.

We now focus on the second and third nanomagnets which are clocked (subjected to electrostatic potentials generating stress) and assume that their magnetizations subtend angles θ_2 and θ_3 with the positive x-axis. The dipole interaction energy of the second nanomagnet is:[13]

$$E_{\text{dipole}} = -\mu_0 \vec{M} \cdot \vec{H}_{\text{dipole}} V = (\mu_0/4\pi R^3)[M_s^2 V^2] \times [-2\cos\theta_2 \cos\theta_3 + (\sin\theta_3 - 1)\sin\theta_2], \quad (1)$$

where μ_0 is the permeability of free space, $\vec{H}_{\text{dipole}}$ is the in-plane magnetic field due to a dipole, and V is the volume of the nanomagnet.

The shape anisotropy energy (energy difference between magnetization along the hard and the easy axis) is[13]:

$$E_{\text{shape-anisotropy}} = (\mu_0/2)[M_s^2 V] N_d, \quad (2)$$

where N_d is the demagnetization factor. We treat the elliptical nanomagnet in the manner discussed by Chikazumi.[13] Its major and minor axis diameters are a and b, while the thickness is t. For the coordinate system consistent with Fig. 1, the expressions for N_d along the y (major axis) and x (minor axis) directions are[13]

$$N_{d\_YY} = \frac{\pi}{4}\left(\frac{t}{a}\right)\left[1 - \frac{1}{4}\left(\frac{a-b}{a}\right) - \frac{3}{16}\left(\frac{a-b}{a}\right)^2\right];$$

$$N_{d\_XX} = \frac{\pi}{4}\left(\frac{t}{a}\right)\left[1 + \frac{5}{4}\left(\frac{a-b}{a}\right) + \frac{21}{16}\left(\frac{a-b}{a}\right)^2\right], \quad (3)$$

provided $a > b$, $a/b \sim 1$ and $a, b > t$.[13]

Since the magnetization of the second nanomagnet subtends an angle θ_2 with the positive x-axis, the shape anisotropy energy can be written as

$$E_{\text{shape-anisotropy}} = \frac{\mu_0}{2}[M_s^2 V](N_{d\_XX}\cos^2\theta_2 + N_{d\_YY}\sin^2\theta_2). \quad (4)$$

Finally, the stress anisotropy energy is[13]

$$E_{\text{stress-anisotropy}} = -\frac{3}{2}[\lambda_s \sigma V]\sin^2\theta_2, \quad (5)$$

where $(3/2)\lambda_s$ is the saturation magnetostriction. Compressive stress will make σ negative and tensile positive.

Using Eqs. (1)–(5), we can write the total energy of the second nanomagnet in Fig. 1 as

$$E_{\text{total-2}} = (\mu_0/4\pi R^3)[M_s^2 V^2][-2\cos\theta_3 \cos\theta_2 + (\sin\theta_3 - 1)\sin\theta_2] + (\mu_0/2)[M_s^2 V](N_{d\_XX} - N_{d\_YY})\cos^2\theta_2 - (3/2)\lambda_s \sigma V \sin^2\theta_2, \quad (6)$$

and similarly the total energy of the third nanomagnet as

$$E_{\text{total-3}} = (\mu_0/4\pi R^3)[M_s^2 V^2][-2\cos\theta_2 \cos\theta_3 + (\sin\theta_2 - 1)\sin\theta_3] + (\mu_0/2)[M_s^2 V](N_{d\_XX} - N_{d\_YY})\cos^2\theta_3 - (3/2)\lambda_s \sigma V \sin^2\theta_3, \quad (7)$$

where we have dropped constant terms which do not depend on θ_2, and/or θ_3.

In order to demonstrate that the magnetizations of the second and third nanomagnets indeed rotate upon application of stress and that the former subsequently settles down in the correct logic state when it is unstressed [indicating that signal has propagated unidirectionally], we have to solve Eqs. (6) and (7) simultaneously to find the energy minima of both nanomagnets as a function of stress applied, with the appropriate initial conditions. An accurate transient solution will require solving the Landau–Lifshitz–Gilbert equations for the coupled system but the final steady-state solution does not require it. All we have to do is minimize $E_{\text{total-2}}$ with respect to θ_2 and minimize $E_{\text{total-3}}$ with respect to θ_3 as we gradually increase and decrease stress adiabatically on the nanomagnets (see Ref. 17 for justification of this procedure). This calculation is carried out numerically.

For the numerical simulation, the multiferroic nanomagnets were assumed to be made of two layers as follows: nickel and lead-zirconate-titanate (PZT) with the following properties: for nickel layer, thickness=10 nm, $(3/2)\lambda_s = -3 \times 10^{-5}$, $M_s = 4.84 \times 10^5$ A/m,[14] and Young's modulus $Y = 2 \times 10^{11}$ Pa. The PZT layer can transfer up to 500×10^{-6} strain to the Ni.[15,16] The major and minor axes of the elliptical nanomagnets are assumed to be $a=105$ nm and $b=95$ nm, respectively, and the center-to-center separation (or pitch) is 160 nm. The above parameters were chosen to ensure that (i) The shape anisotropy energy barrier of the nanomagnets $K_u V = \mu_0/2[M_s^2 V](N_{d\_YY} - N_{d\_XX})$ is sufficiently high ($\sim$0.8 eV or $\sim 32\ kT$ at room temperature) so that the bit error probability due to spontaneous magnetization flipping is very low ($\sim e^{-32} \approx 10^{-14}$). (ii) The stress anisotropy energy ($\sim$1.5 eV) generated in the magnetostrictive Ni layer due to a strain of 500×10^{-6} transferred from the PZT layer can rotate the second magnet out of the initial state so that upon removal of the stress, it flips to the correct state as shown in Fig. 1. (iii) The dipole interaction energy is limited to 0.2 eV which is significantly lower than the shape anisotropy energy. This prevents the magnetization from switching spontaneously without the application of the electric-field induced stress.

Equations (6) and (7) are evaluated as functions of orientations θ_2 and θ_3 to find the energy minima. Initial conditions are $\sigma=0$, $\theta_2=-90°$, and $\theta_3=+90°$ corresponding to the top row of Fig. 1. For each increment in stress, the new θ_2 and θ_3 are simultaneously evaluated. Furthermore, it is assumed that both magnetization orientations rotate to the right to simplify the numerical analysis. The analysis would be identical if both magnetizations rotated to the left because of

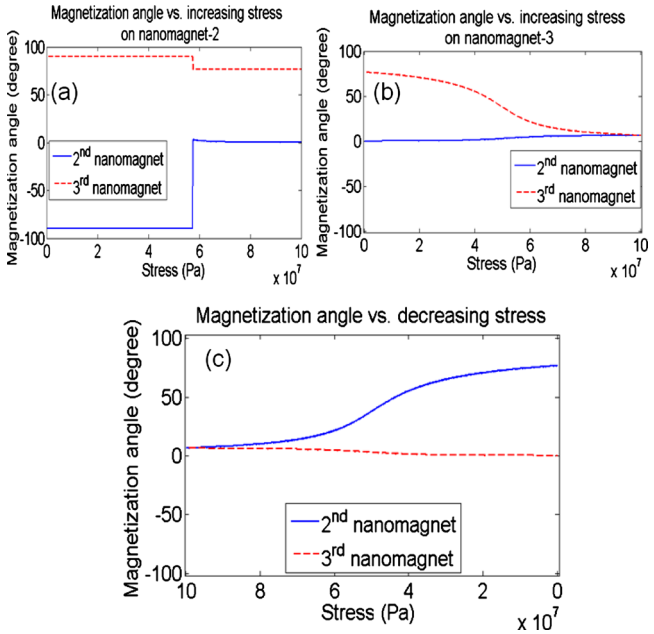

FIG. 2. (Color online) Rotation angle θ_2 of the second nanomagnet and θ_3 of the third nanomagnet as a function of stress. (a) For increasing stress applied to the second nanomagnet while the third nanomagnet is not stressed (b) for increasing stress applied to the third nanomagnet while a constant stress of 100 MPa is maintained on the second nanomagnet (c) for decreasing stress on the second nanomagnet to zero while a constant stress of 100 MPa is maintained on the third nanomagnet.

the symmetry. We first rotate the second nanomagnet by applying stress to it and then rotate the third nanomagnet. This ensures that the probability of one magnet rotating to the left and the other rotating to the right is very small because the x-component of $\vec{H}_{\text{dipole}}$ on the third nanomagnet exceeds the y-component when the second nanomagnet has already completed its rotation through a large angle. The x-component favors lining up the rotated magnetizations in the same direction (parallel) while the y-component favors lining them up in opposite directions (antiparallel).

In Fig. 2(a), we plot θ_2 and θ_3 as a function of tensile stress applied on the second nanomagnet while the third nanomagnet is left unstressed. Surprisingly, there is no rotation in both θ_2 and θ_3 for small values of stress. But at a certain threshold stress [$\sim$58 MPa], the second magnet switches abruptly from $\theta_2=-90°$ to $\theta_2=+6°$ while the third nanomagnet switches abruptly from $\theta_3=+90°$ to $\theta_3=+75°$. Even though the third magnet is unstressed, it rotates because the second magnet's rotation away from $-90°$ immediately causes an x-component of $\vec{H}_{\text{dipole}}$ to appear on the third magnet which then makes it rotate. Further increase in stress on the second magnet has little effect on θ_3 but θ_2 decreases asymptotically to 0° when the stress is increased to 100 MPa.

In Fig. 2(b), we plot θ_2 and θ_3 when stress is held constant at 100 MPa on the second nanomagnet and gradually increased on the third nanomagnet. There is no abrupt switching of magnetization. Gradually θ_3 decreases from +75° to +6° while θ_2 increases from close to 0° to +6°. At this point, the initial antiparallel configuration of the second and third nanomagnet has become parallel as one magnetization has rotated clockwise and the other anticlockwise (both have rotated to the right) to reach a final state of $\theta_2 = \theta_3 = 6°$. Both magnetizations have rotated by nearly 90° from their initial orientation upon being subjected to a stress of 100 MPa.

Finally, in Fig. 2(c) we plot θ_2 and θ_3 as a function of decreasing stress on the second magnet while the third is maintained at a constant stress of 100 MPa. The second nanomagnet gradually rotates into the "nearly-up" state ($\theta_2 \approx 80°$) while the third nanomagnet aligns approximately along the hard axis ($\theta_3 \approx 0.2°$). Thus, at the end of the stress cycle on the second nanomagnet, the latter has flipped from its initial "down" state to the nearly "up" state. Repeating this sequence on the next pair of nanomagnets (third and fourth) propagates the input logic bit (magnetization orientation of the first nanomagnet) down the chain. In this fashion, Bennett clocking is successfully implemented.

We also investigated the cases when stress was applied simultaneously on both nanomagnets, as well as sequentially on the third followed by the second (see the supplement, Ref. 17). A deeper physical understanding of the magnetization rotation can be gained by looking at the energy profiles of the second and third nanomagnets as a function of θ_2 and θ_3 (Figs. S3–S5 in the supplement, Ref. 17) at zero and other intermediate stresses.

In conclusion, we have shown that nanomagnets can be electrically switched for Bennett clocking. Using the piezoelectric coefficient of PZT ($d_{31} \sim -100 \times 10^{-12}$ m/V), a voltage of only 0.2 V will be required to induce a stress of 100 MPa in a 40 nm PZT layer, assuming linear behavior. This results in very low energy dissipation. Preliminary experiments to demonstrate such switching has been reported in the literature, although not in single domain nanomagnets.[18] This method of clocking is superior to using a local magnetic field to rotate the magnetic moment[19] since a magnetic field cannot be confined easily to dimensions of $\sim$100 nm (cell size). It also has potential to be more energy-efficient[17] than spin transfer torque for switching nanomagnets.[5] Curiously, the energy dissipated in switching a magnet is a tiny fraction of the energy expended in the clock,[17] so that it is imperative to focus research on improving the clocking methodology rather than magnet switching.

[1]R. P. Cowburn and M. E. Welland, Science **287**, 1466 (2000).
[2]G. Csaba *et al.*, IEEE Trans. Nanotechnol. **1**, 209 (2002).
[3]B. Behin-Aein *et al.*, IEEE Trans. Nanotechnol. **8**, 505 (2009).
[4]S. Salahuddin and S. Datta, Appl. Phys. Lett. **90**, 093503 (2007).
[5]B. Behin-Aein *et al.*, Nat. Nanotechnol. **5**, 266 (2010).
[6]S. Bandyopadhyay and M. Cahay, Nanotechnology **20**, 412001 (2009).
[7]D. B. Carlton *et al.*, Nano Lett. **8**, 4173 (2008).
[8]F. M. Spedalieri *et al.*, arXiv:0906.5172v1 (unpublished).
[9]C. H. Bennett, Int. J. Theor. Phys. **21**, 905 (1982).
[10]W. Eerenstein *et al.*, Nature (London) **442**, 759 (2006).
[11]C. Nan *et al.*, J. Appl. Phys. **103**, 031101 (2008).
[12]J. Atulasima *et al.*, J. Appl. Phys. **103**, 014901 (2008).
[13]S. Chikazumi, *Physics of Magnetism* (Wiley, New York, 1964).
[14]E. W. Lee, Rep. Prog. Phys. **18**, 184 (1955).
[15]M. Lisca *et al.*, Appl. Surf. Sci. **252**, 4549 (2006).
[16]T. Watanabe *et al.*, J. Electrochem. Soc. **155**, D715 (2008).
[17]J. Atulasimha and S. Bandyopadhyay, arXiv:1005.5358v1 (unpublished); See supplementary material at http://dx.doi.org/10.1063/1.3506690 discussing all other switching cases and energy profiles.
[18]T. Brintlinger *et al.*, Nano Lett. **10**, 1219 (2010).
[19]M. T. Alam *et al.*, IEEE Trans. Nanotechnol. **9**, 348 (2010).